Supplementary methods, table, figures, references:

The crystal structure of AphB, a virulence gene activator from *Vibrio cholerae,* reveals residues that influence its response to oxygen and pH

Taylor, et al.

Supplementary methods

Size exclusion chromatography

Purified protein samples were applied to a Superdex 200 10/300 GL column (GE Life Sciences) at a flow rate of 0.5 mL min^{-1} in PBS buffer and absorbance at 280 nm was monitored. Although molecular weight standards were used to calibrate this column, the molecular weight calculated from the retention volume of AphB (179,800 kDa) was much greater than that of the tetramer (133,285 kDa). However, the crystal structure of AphB clearly reveals that the tetramer is ellipsoidal rather than spherical. Since the dimensions of the tetramer are 108 Å x 87 Å x 64 Å, the protein was treated as an oblate ellipsoid with a semimajor axis, a = 97.5 Å (the average of the two longest dimensions) and a minor axis, b = 64 Å. To determine the radius of a sphere equal in volume to AphB (R_{sphere}), the following equation was used:

(1) $R_{sphere} = (\alpha^2 \beta)^{1/3}$

where α=48.75 Å (half the semimajor axis, a) and β = 32 Å (half the minor axis, b). Thus, R_{sphere} = 42.4 Å. Since Stokes radius $\propto$ K_{av}, the corrected partition coefficient ($K_{av(sphere)}$) can be calculated using the ratio of R_{sphere} to the semimajor axis of AphB (48.75 Å).

(2) $(48.75 \text{ Å} \times K_{av(ellipse)}) / 42.4 \text{ Å} = K_{av(sphere)} = 0.33$

Extrapolation from the standard curve of log(MW) vs. K_{av} reveals a corrected molecular weight of 135 kDa for AphB.

Analytical ultracentrifugation studies

Experiments were conducted in an XI-analytical ultracentrifuge (BeckmanCoulter) with an AN-60 TI rotor. Experiments for wild-type AphB were performed using a buffer containing the 20 mM Tris pH 8.0, 100 mM NaCl and 1 mM EDTA (physiological salt concentration) as well as in crystallization buffer (20 mM Tris pH 8.0, 500 mM NaCl and 1 mM EDTA). Purified wild-type AphB in concentrations of 17.2, 8.6 and 4.3 μM was loaded into six-sector cells with 1.2 cm path length for each buffer condition. Absorbance at 280 nm was recorded. SEDNTERP (Laue *et al*., 1992) was used to calculate partial specific volume from amino acid sequence and solvent density from buffer composition. The resulting data sets were preprocessed and fit to monomer, dimer, tetramer and tetramer-octamer models in SEDANAL (Stafford and Sherwood, 2004). The best fit for both sets of wild-type data was attained with a tetramer-octamer model, and this fit was confirmed to 99% confidence with F-statistics. Although the calculated concentration of octamer in solution is low (1%, an association constant of 10^{-4} was determined from processed data) formation compared to that of the tetramer, it is interesting to note that in the lower-resolution (4.0 Å) crystal form of wild-type AphB, the protein packs as an octamer in the crystal lattice (Fig. S5).

Table S1. Data collection and refinement statistics

	SeMet AphB-CTD
Data collection	
Space group	P 3_2 2 1
Cell dimensions	
a, *b*, *c* (Å)	112.3, 112.3, 88.9
α, β, γ (°)	90, 90, 120
Resolution (Å)	97.5- 2.2 (2.5-2.2)
R_{meas}	0.11 (0.49)
$I/\sigma I$	16.1 (4.0)
Completeness (%)	98.2 (97.8)
Redundancy	5.8 (5.9)

TABLE S2. Oligonucleotides used in this study

Name	**Sequence (5'-3')**
CO2-52	GATCGGCTCTTCAACCATGATCCCTGTGGCAACG
CO2-53	GATCGGCTCTTCAGGTCTTCTTTGAAGTTGAGGTATAGCTTCC
BP98DF	ATTCGTATTTCTGCAGATTCCAATCTGACAAAACG
BP98DR	CGTTTTGTCAGATTGGAATCTGCAGAAATACGAATGC
BN100EF	TATTTCTGCACCATCCGAACTGACAAAACGAATGATG
BN100ER	TCATTCGTTTTGTCAGTTCGGATGGTGCAGAAATACG
BL101EF	TCTGCACCATCCAATGAAACAAAACGAATGATG
BL101ER	CATCATTCGTTTTGTTTCATTGGATGGTGCAGA
BL101NF	TCTGCACCATCCAATAACACAAAACGAATGATG
BL101NR	CATCATTCGTTTTGTGTTATTGGATGGTGCAGA
BL101NF	TCTGCACCATCCAATAACACAAAACGAATGATG
BL101NR	CATCATTCGTTTTGTGTTATTGGATGGTGCAGA
BN128EF	GAGCTGATGATGAGTGAACAAGCCGACGATCTC
BN128ER	GAGATCGTCGGCTTGTTCACTCATCATCAGCTC
BV144EF	GATGTGATTTTCCGAGAAGGCCCACAGCGTGATTCC
BV144ER	GGAATCACGCTGTGGGCCTTCTCGGAAAATCACATC
BY192AF	CAGTTGCTCAAAGGTGCGCCATTGCTCAAATGG
BY192AR	CCATTTGAGCAATGGCGCACCTTTGAGCAACTG
BP193DF	GTTGCTCAAAGGTTATGATTTGCTCAAATGGCAAC
BP193DR	GTTGCCATTTGAGCAAATCATAACCTTTGAGCAAC
BP193AF	GTTGCTCAAAGGTTATGCGTTGCTCAAATGGCAAC
BP193AR	GTTGCCATTTGAGCAACGCATAACCTTTGAGCAAC
BL194EF	CTCAAAGGTTATCCAGAACTCAAATGGCAACTG
BL194ER	CAGTTGCCATTTGAGTTCTGGATAACCTTTGAG
BL220EF	TTTCAAGCCAGCGCAGAAAATGTTGTTCGCAGC
BL220ER	GCTGCGAACAACATTTTCTGCGCTGGCTTGAAAACG
BC227SF	GTTGTTCGCAGCGCATCTTCAGAAGGTTTAGGC
BC227SR	GCCTAAACCTTCTGAAGATGCGCTGCGAACAAC
BP237DF	GGCATTACGCTCATGGATGATGTGATGCTGCGTG
BP237DR	ACGCAGCATCACATCATCCATGAGCGTAATGCC
BM240ER	CTCATGCCCGATGTGGAACTGCGTGAATTTCTTG
BM240ER	CAAGAAATTCACGCAGTTCCACATCGGGCATGAGC
BR262EF	TTGGAGCTCAAACCCGGAAGATATCTACATGCTGTATAAC
BR262ER	ACAGCATGTAGATATCTTCCGGGTTTGAGCTCCAATC

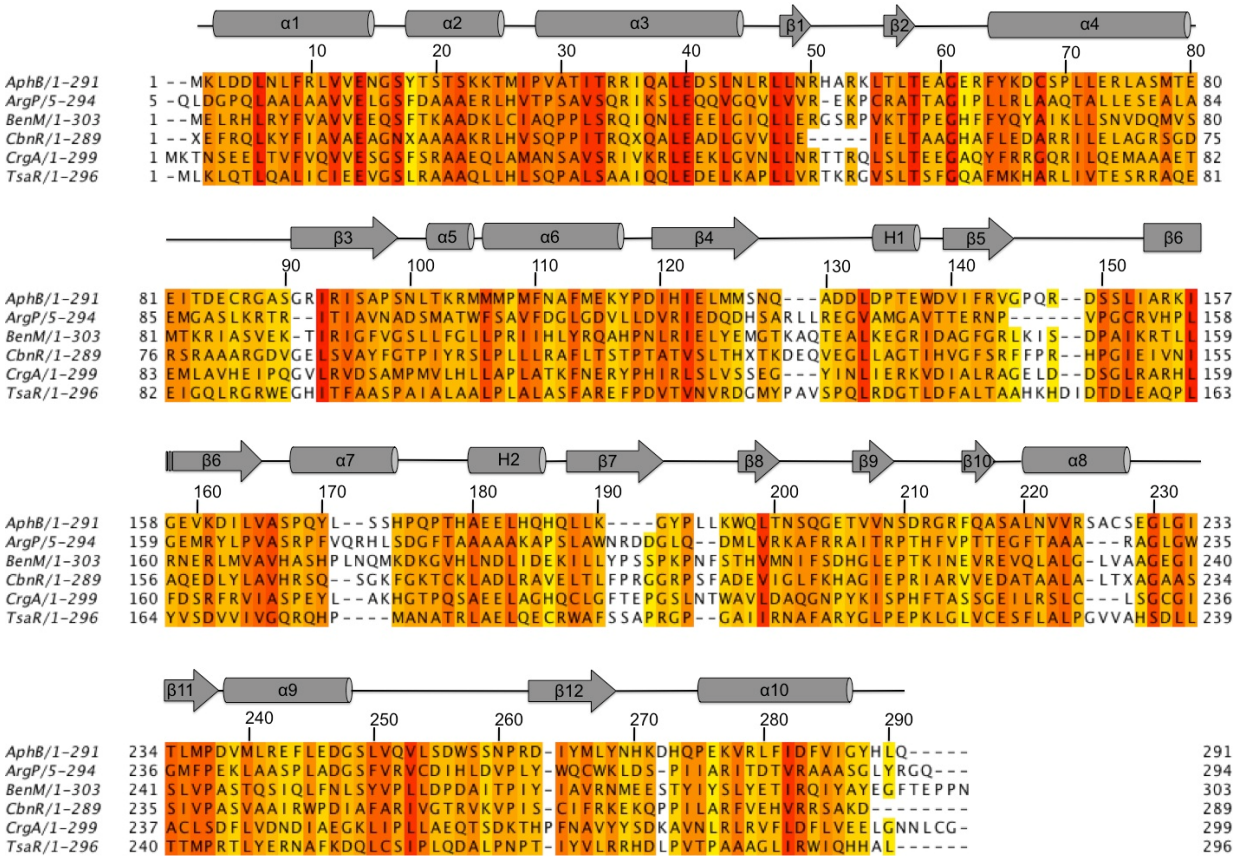

Fig. S1. Alignment of the sequences of five other full-length LTTR proteins with AphB. For AphB, residues 1-58 comprise the DNA binding domain, residues 59-89 comprise the linker helix, and residues 90-291 comprise the regulatory domain. ClustalW (Larkin *et al*., 2007) alignments were rendered in JalView (Clamp *et al*., 2004) and colored according to percent identity. The residues in the red boxes show the highest identity and the residues in the yellow boxes show the least identity.

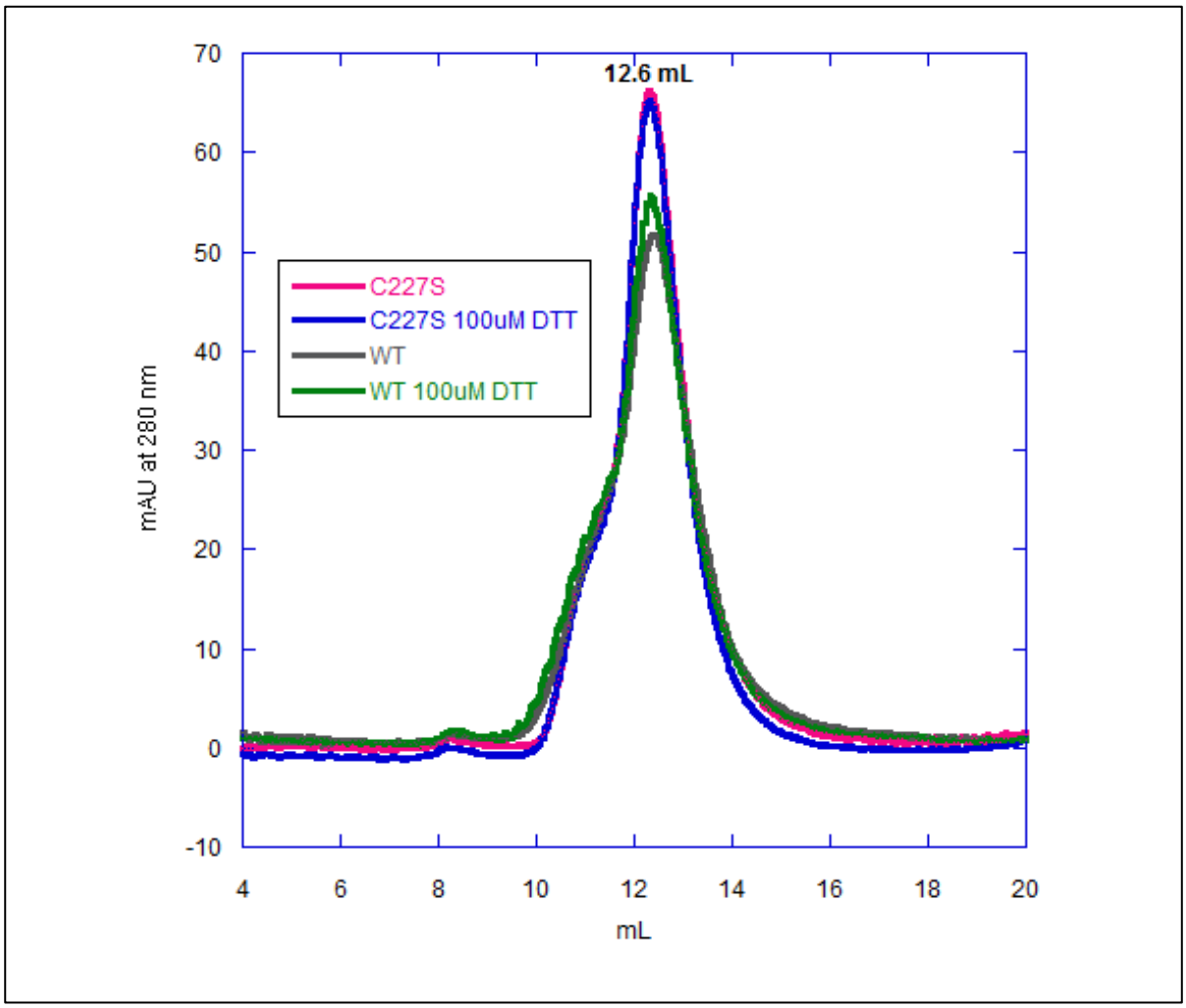

Fig. S2. Gel filtration analysis of wild-type and AphB C227S in the presence and absence of reducing agent. The retention volumes of WT AphB, grown aerobically and purified in the absence of reducing agent, are the same regardless of the presence (green) or absence (gray) of 100 uM DTT in the injected sample. The retention volume of 12.6 mL on a calibrated Superdex 200 size exclusion column indicates that the protein is tetrameric in both samples. These experiments were repeated for C227S AphB with (blue) and without (magenta) 100 uM DTT and it was observed that this AphB variant is also tetrameric under reducing and nonreducing conditions.

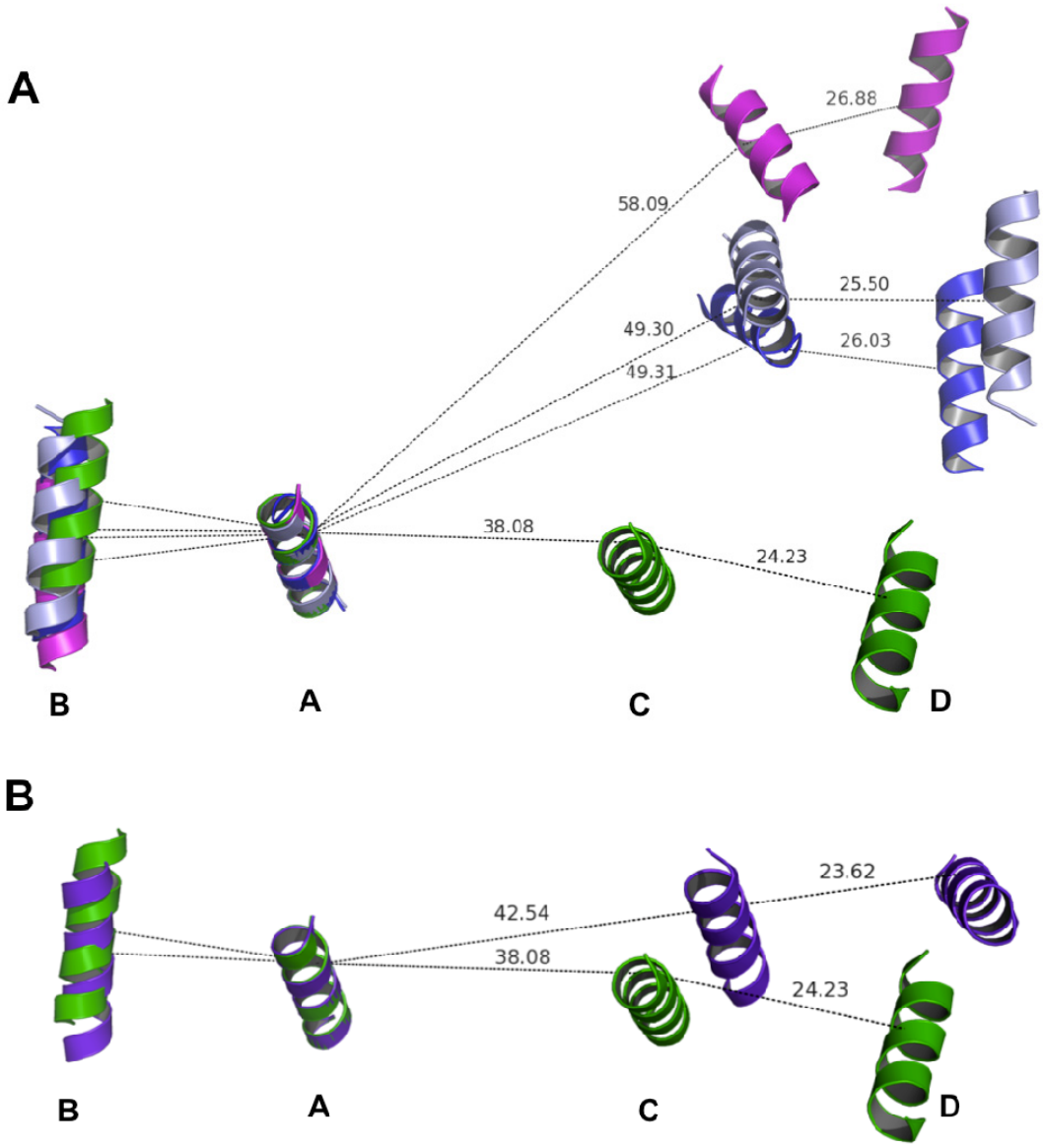

Fig. S3. Positioning of recognition helices (α3) in LTTR tetramers. (A) Alignment of the recognition helices of AphB (green), ArgP (silver), CbnR (magenta) and TsaR (blue) by a superposition of the recognition helix of subunit A of each tetramer onto that of AphB. (B) Superposition of the recognition helix of subunit A of N100E AphB (purple) onto that of wild-type AphB (green).

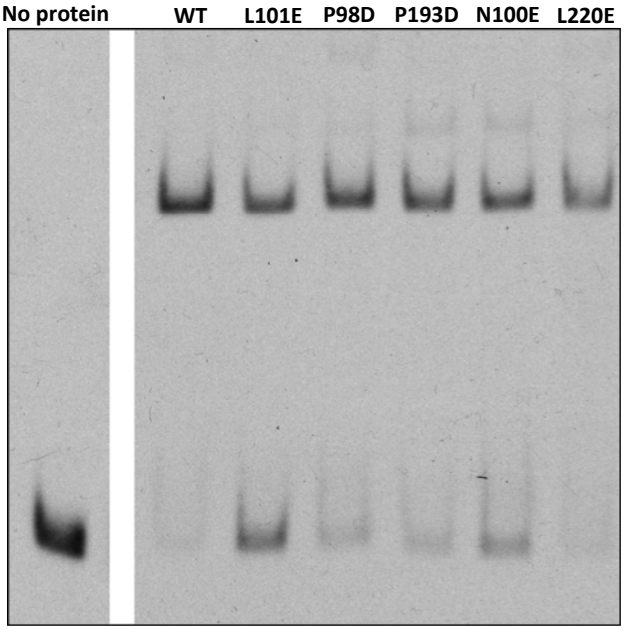

Fig. S4. Gel mobility shift assay showing binding of wild-type (WT) and mutant AphB proteins to a *tcpPH* promoter fragment (-175 to -40 with respect to the start of transcription). The *tcpPH* promoter fragment with no protein is shown at left. Samples containing the same fragment with WT AphB and AphB variants, as labeled, are shown at right. Lanes with WT and variant AphB each contain 320 nM protein. The DNA fragment was amplified by PCR (Kovacikova & Skorupski, 2002) and end labeled with digoxygenin (Kovacikova & Skorupski, 2001). The binding reactions were carried out as previously described (Kovacikova & Skorupski, 2001).

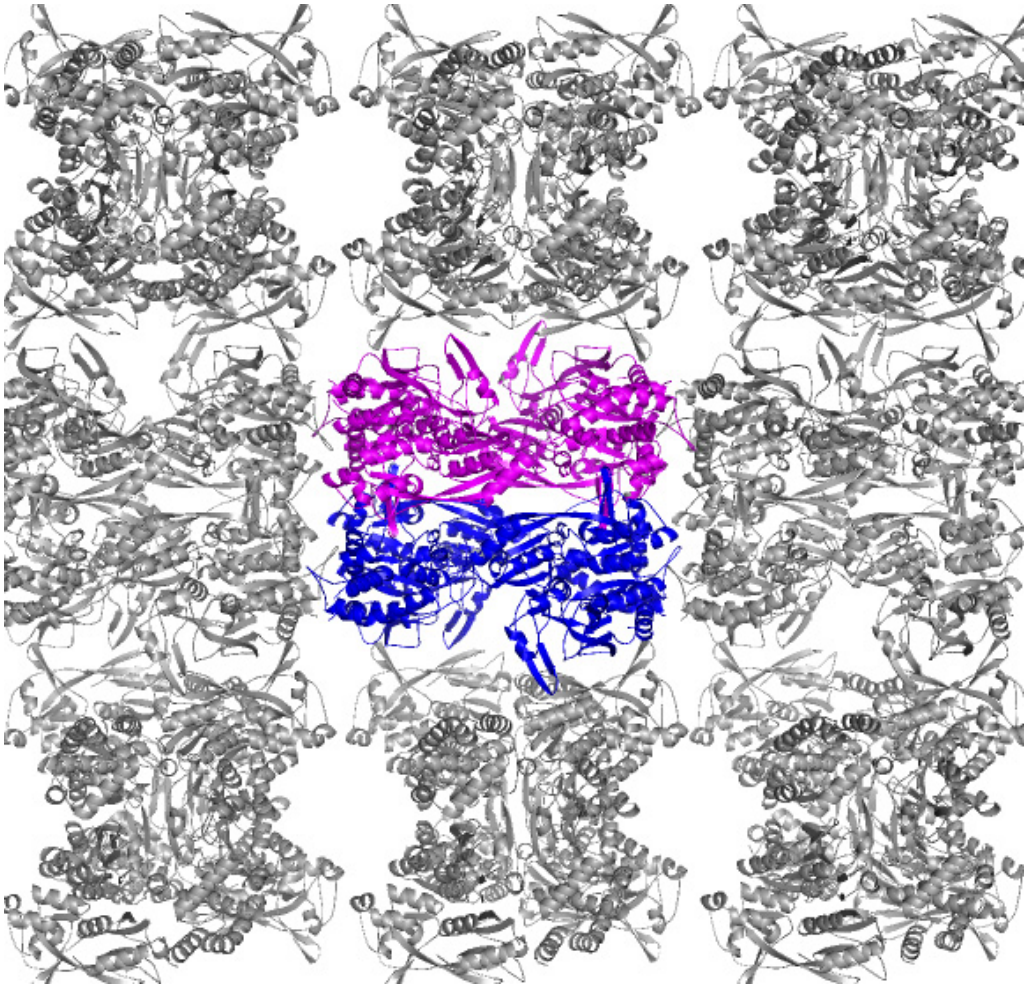

Fig. S5. Packing diagram of the molecular replacement solution for AphB WT crystal form I. Under the same crystallization conditions, WT AphB crystallized in a high-resolution orthorhombic crystal form (form II) and a lower-resolution tetragonal crystal form (form I). In the crystal lattice of form I, two equivalent tetramers (blue and magenta, above) pack face-to-face, with the DNA-binding domains located on the inside of the octameric assembly.

References

Clamp, M., Cuff, J., Searle, S. M., and Barton, G. J. (2004). The Jalview Java alignment editor. *Bioinformatics* **20:** 426–427.

Kovacikova, G., and Skorupski, K. (2001). Overlapping binding sites for the virulence gene regulators AphA, AphB and cAMP-CRP at the *Vibrio cholerae tcpPH* promoter. *Mol Microbiol* **41:** 393-407.

Kovacikova, G., and Skorupski, K. (2002). Binding site requirements of the virulence gene regulator AphB: differential affinities for the *Vibrio cholerae* classical and El Tor *tcpPH* promoters. *Mol Microbiol* **44:** 533–547.

Larkin, M. A., Blackshields, G., Brown, N. P., Chenna, R., McGettigan, P. A., McWilliam, H., Valentin, F., *et al.* (2007). Clustal W and Clustal X version 2.0. *Bioinformatics* **23:** 2947-2948.

Laue, T.M., Shah, B.D., Ridgeway, T.M., and Pelletier, S.L. (1992). Computer-aided interpretation of analytical sedimentation data for proteins. In *Analytical Ultracentrifugation in Biochemistry and Polymer Science*. Harding, S.E., Rowe, A.J. & Horton, J.C. (eds), Cambridge, UK: The Royal Society of Chemistry, pp. 90–125.

Stafford, W. F., and Sherwood, P. J. (2004). Analysis of heterologous interacting systems by sedimentation velocity: curve fitting algorithms for estimation of sedimentation coefficients, equilibrium and kinetic constants. *Biophys Chem* **108:** 231–243.